International Journal of Psychophysiology 167 (2021) 57–68

Contents lists available at ScienceDirect

International Journal of Psychophysiology

journal homepage: www.elsevier.com/locate/ijpsycho

Decoding of cognitive processes involved in the continuous performance task

Fariba Sharifian *, Daniel Schneider, Stefan Arnau, Edmund Wascher

Leibniz Research Centre for Working Environments and Human Factors (IfADo), Department of Ergonomics, Ardeystr. 67, 44139 Dortmund, Germany

ARTICLE INFO

Keywords:
Continuous performance task
Multivariate pattern analysis
Electroencephalogram
Classification
Cognitive functions

ABSTRACT

Decoding of electroencephalogram brain representations is a powerful data driven technique to assess the stream of cognitive information processing. It could promote a more thorough understanding of cognitive control networks. For many years, the continuous performance task has been utilized to investigate impaired proactive and reactive cognitive functions. So far, mainly task performance and univariate electroencephalogram were involved in such investigations. In this study, we benefit from multi-variate pattern analysis of continuous performance task variations to provide a more complete spatio-temporal outline of information processing flow involved in sustained and transient attention and response preparation. Besides effects that are well in line with previous EEG research but could be described in more spatial and temporal detail by the used methods, our results could suggest the presence of a higher order feedback control system when expectations are violated. Such a feedback control is related to modulations of behavior both intra- and inter-individually.

1. Introduction

The Electroencephalogram (EEG) has been extensively used to study the neurocognitive basis underlying the behavioral results in neurocognitive tasks. These studies usually focus on the univariate analyses, (Luck, 2014) for example based on event-related potentials (ERP). However, such univariate analysis of the EEG signal relies on some hypothesis about specific ERP components and their associations with specific cognitive functions. This means that the traditional ERP analysis would be limited to some pre-defined hypothesis. On the other hand, multi variate pattern analysis (MVPA) of the whole-brain EEG signal allows us to decode different experimental conditions based on the observed patterns of brain responses with minimum a-priori assumptions about a specific electrode or timing (Lotte et al., 2018; Fahrenfort et al., 2018; Cichy and Pantazis, 2017; Alizadeh et al., 2017). In addition, MVPA of the EEG signal provide a tool to look at the temporal dynamics of the neural activation pattern (Fahrenfort et al., 2018). Moreover, by MVPA it is possible to correlate different physiological or behavioral measures with the neural activation patterns (Fahrenfort et al., 2017; Fahrenfort et al., 2018).

The Continuous Performance Task (CPT, (Halperin, 1991; Rosvold et al., 1956)) has been widely used to investigate neural cognitive dysfunctions in many mental diseases such as learning disorders (Dhar et al., 2010), attention-deficit hyperactivity disorder (ADHD, (Slobodin, 2020; Nichols and Waschbusch, 2004)) and schizophrenia (Cohen and Servan-Schreiber, 1992; Elvevåg et al., 2000; Servan-Schreiber et al., 1996). Usually, task scores such as accuracy rate, response time, omission and commission errors are considered as indicators of overall task performance. However, in order to effectively make use of CPT in clinics, it is necessary to have a clear understanding of what cognitive functions are involved and respectively influence the task performance (Borgaro et al., 2003; Riccio et al., 2002). MVPA enables us to decode and characterize the time course of cognitive functions involved in the CPT at each stage of information processing.

Classically, in the CPT, subjects need to detect one specific rare letter among others letters in a sequence and report it by pressing a button. For example, random combinations of letters A / B and X / Y were presented and the subjects need to press a response button whenever an X letter appears on the screen. This classical version, usually called X-CPT (Rosvold et al., 1956), demands sustained attention and preparation of motor related functions only based on the target stimulus (Smid et al., 2006). Several different versions of CPT exist, each engaging particular cognitive functions and requiring specific task interpretation (Eimer, 1996, 1997). In a popular version of CPT, named AX-CPT (Cohen et al., 1999), subjects should only report the target letter, if it is preceded by a pre-defined cue in the sequence of letters. Back to the example, the

* Corresponding author.
E-mail address: sharifian@ifado.de (F. Sharifian).

https://doi.org/10.1016/j.ijpsycho.2021.06.012
Received 8 February 2021; Received in revised form 22 June 2021; Accepted 25 June 2021
Available online 1 July 2021

subjects need to press a response button whenever an X letter appears after an A letter. This cue-target combination is rare in the experiment. The AX-CPT requires the participants to maintain goal-relevant information from the previous stimulus in working memory to be able to decide whether to respond or not (Barch et al., 2001; Servan-Schreiber et al., 1996). A large number of modified versions of the X-CPT and AX-CPT have been used, with different frequencies of target stimuli and cue-target combinations.

It has been proposed, that there are two distinct cognitive control networks for reactive and for proactive cognitive control (Braver et al., 2009). In the case of reactive cognitive control, the cognitive functions are activated only when they are demanded, whereas with proactive cognitive control, cognitive functions relevant to the task are activated in advance of an explicit need of them (Braver, 2012). There are various theories about how reactive and proactive cognitive control is performed during a CPT (Mäki-Marttunen et al., 2019). Smid et al. (2006) suggested that not just single dimensions of cognitive functions, but a two-dimensional operation of attention and response preparation drive reactive vs. proactive cognitive control. These main cognitive dimensions are also hypothesized to be related to working memory (Richmond et al., 2015; Smid et al., 2006; Barch et al., 2001) and include the ability to temporary keep information about a specific stimulus/sequence of stimuli to decide about the correct response. While the X-CPT asks for sustained attention to a single predefined stimulus (for example the letter X), the AX-CPT needs attention to switch based on the cue information (the A cue tells if X is a target letter). Such switches of attention, specifically when focused on a specific stimulus feature (e.g. color or shape (Eimer, 1997)), is known to increase working memory load (Barch et al., 2001; Servan-Schreiber et al., 1996). As a consequence, task performance was found to be decreased in the AX-CPT compared to the X-CPT (Smid et al., 2006; Wascher et al., 2020; Borgaro et al., 2003; Coons et al., 1981). The second dimension of cognitive functions is related to motor functions (Fallgatter, 2001; Ornitz et al., 2001) and includes the ability to prepare for a response. The classical X-CPT request for sustained response preparation as every stimulus can be a potential target. However, in the AX-CPT, the cue gives information about whether the next stimulus is a potential target or not. Therefore, the AX-CPT allows for transient response preparation. It has been shown that response times decrease when response preparation is based on cue information, which is the case in AX-CPT compared to X-CPT (Smid et al., 2006; Wascher et al., 2020; Dias et al., 2003). CPT versions with different probabilities of cue/target combinations (Richmond et al., 2015; Wascher et al., 2020) include statistical learning which might also affect whether allocation of attention and motor preparation is engaged in a rather proactive or reactive way.

The cognitive functions involved in different versions of the CPT have been investigated in previous univariate EEG studies. It could be shown that selection negativity (SN) features significantly larger amplitudes in the X-CPT than in the AX-CPT (Smid et al., 2006; Eimer, 1997; Smid et al., 1999). SN results from subtracting ERPs of stimuli with target-irrelevant from the stimuli with target-relevant feature. SN is most pronounced at recording sites over visual areas and usually starts 140 ms after stimuli onset. It has been suggested that an increased SN latency and decreases in SN amplitude are associated with impaired target detection at early stage of visual processing (Eimer, 1996, 1997; Smid et al., 1999). In addition, Contingent Negative Variation (CNV) was only reported for the target relevant cue in AX-CPT and not following an target irrelevant cue (Smid et al., 2006). The CNV can be observed at around 500 ms after stimulus onset over the central areas and is hypothesized to reflect cognitive or motor preparation (Ulrich et al., 1998; Brunia, 1993). The Lateralized Readiness Potential (LRP) onset latency (Hackley et al., 1990; Smid et al., 2000; Leuthold et al., 1996) also indicates response preparation. The LRP is evoked faster in the AX-CPT compared to the X-CPT (Smid et al., 2006). SN reflects visual selective processing of attended stimuli and both CNV and LRP show proactive response preparation. However, as mentioned earlier, these findings are limited on the hypothesis about some ERP components and their associations with specific cognitive functions.

In the present study, we aimed for an integrated map of sensory and cognitive processes involved in sustained/transient attention and response preparation in the CPT task. We used a linear classifier (Cristianini and Shawe-Taylor, 2000) and executed spatial and temporal decoding of the EEG signal in the CPT conditions. We performed variations of X-CPT and AX-CPT experiments (Richmond et al., 2015; Wascher et al., 2020) with fixed global and varying local probability of both cue and probe appearances. This means, each pair of relevant cue-target (i.e. A-X letters combination) and irrelevant cue – nontarget (i.e. B–Y letters combination) appeared 40% of the trails in the tasks, while the other two pairs of relevant cue – nontarget (i.e. A–Y letters combination) and irrelevant cue – target (i.e. B-X letters combination) each appeared in only 10% of trials. In our design, both A and B -cue have comparable novelty and validity for probe prediction. In addition, both target and non-target probes are expected with the same probability, and as a result one response is not more likely than the other one. Correspondingly, our CPTs differentiated between sustained and transient target detection (i.e. X-CPT vs. AX-CPT), as well as between implicit (i.e. from statistical learning of cue-probe association) and implicit-explicit (i.e. both implicit by cue-target combination frequencies and explicitly by task instructions) response preparation (again i.e. X-CPT vs. AX-CPT). Specifically, we tried to classify target relevant vs. target irrelevant cues in case of implicit (A vs. B -cue in X-CPT) and implicit-explicit (A vs. B -cue in AX-CPT) association with target. By that, we aim to decode proactive cognitive control starting after cue onset derived from implicit vs. explicit information. In addition, we tried to find out how target-probes vs. nontarget-probes are decodable in task conditions requiring sustained (AX vs. BY -probe in X-CPT) compared to transient attention (AX vs. BY -probe in AX-CPT). In particular, the target detection and proactive response programing could show different timing in these conditions. Moreover, we aimed to detect the effect of implicit vs. implicit-explicit target relevant cue on target-probes (AX-probe in X-CPT vs. AX -probe in AX-CPT) and nontarget-probes (AY-probe in X-CPT vs. AY-probe in AX-CPT). We expect to be able to decode sustained vs. transient attention and track the flow of information over time as well as being able to locate the cognitive functions involved in sensor space. In addition, we hypothesize that implicit vs. implicit-explicit response preparation generates decodable brain activity, and specifically expect to see that over the prefrontal areas (Fallgatter, 2001). Moreover, we assume that the state of the brain while dealing with relevant cue – nontarget (i.e. A-Y letters combination) and irrelevant cue – target (i.e. B-X letters combination) can provide advantageous information about neural interaction involved in response inhibition in healthy brains, and such information can provide a reference to be compared to in the clinical conditions.

2. Methods

2.1. Participants

The investigation is part of the 'Dortmund Vital Study' Project. The Dortmund Vital Study Project is a two days lasting evaluation that includes collection of multi-dimensional data to study interaction between human biological processes and environmental factors over the participants' life span. We analyzed data from 460 healthy subjects (176 male) with an average age of 43.96 ± 13.73 years (age range: 20–70 years) with no history of neurological, cardiovascular, oncological or psychiatric diseases. 17 subjects (2 males; average age: 49.71 ± 12.39; age range: 25–67) were removed from the analysis due to EEG preprocessing criteria (see EEG recording section). 29 further subjects (13 males; average age: 45.14 ± 12.90; age range:20–67) were removed due to poor task performance (more than 50% commission or omission errors in one of the tasks) except for the analysis that are focused on the task performance relationship with the neural activation patterns (i.e. Fig. 7).

Participants provided informed written consent prior to the study and were reimbursed with 160 € for the two days procedure. The ethics committee of the Leibniz Research Centre for Working Environment and Human Factors (Dortmund, Germany) approved the study.

2.2. Procedure

Subjects were seated in a sound attenuated room on a comfortable armchair. Stimuli were presented on a 32 in., 1920 × 1080 pixels VSG monitor (Display++ LCD, M0250 & M0251) with 100 Hz refreshing rate Force sensitive handles recorded manual responses. The sequence of presentation and stimuli were generated with FreePascal software (https://www.freepascal.org/).

The letters A or B were used as the cues, and X or Y as the probes. The letters were presented in gray color on a black background with height of 1° visual angle. The sequence of each task trial (Fig. 1) consisted of: 1) the cue (i.e. letter A or B) for 150 ms, 2) the inter stimuli interval (ISI) with a fixation cross at the center of the screen for 1850 ms, 3) the probe (i.e. letter X or Y) for 150 ms, and 4) the inter stimuli interval with a fixation cross at the center of the screen with a time window for responding of 1850 ms.

Our experiment consisted of two main tasks: X-CPT and AX-CPT. For all the subjects, AX-CPT was performed before X-CPT. In the X-CPT, subjects were instructed to respond to the X-probe as a target regardless of the cue. In the AX-CPT, subjects were asked to respond to the X-probe only if it was preceded by an A-cue.

Each task consisted of 240 trials. In both tasks, all the letters had an equal probability to appear globally but had different local probabilities. This means that the cue-probe pairs of AX and BY had a probability of 40% while each cue-probe pair of AY and BX were less probable with only 10% appearance. The probes are labeled 'AX-probe', meaning an X probe following an A-cue, and 'BX-probe', meaning an X probe preceded by a B-cue. Likewise, 'AY-probe' means an Y probe following an A-cue, and BY-probe means a Y probe preceded by a B-cue. The participants were asked to respond with the thumb of the right hand to the targets. The subjects were also instructed to respond as quickly and accurately as possible. The behavioral responses were collected with a force key and were divided into correct responses, misses (omission errors), correct no-go trials without a response, or false responses in trials not requiring a response (commission errors).

2.3. EEG recording

The EEG data were recorded by means of a BrainVision Brainamp DC amplifier and BrainVision Recorder software (BrainProducts GmbH). The data were acquired with 1000 Hz sampling rate and were filtered online using a 200 Hz low-pass filter. We collected the signal by a 64-channel elastic cap arranged based on the 10–20 system, with FCz electrode as the on-line reference electrode. The preprocessing pipeline was based on EEGLAB (Delorme and Makeig, 2004) and MATLAB (MathWorks Inc. MATLAB, 2019a). The pipeline consisted of re-referencing the signal to the global average of all electrodes and high-pass filtering to 0.1 Hz. Next, bad channels were removed by using EEGLAB. ICA was used in order to detect artifacts. For that, EEG data were down-sampling to 250 Hz, filtered with a bandpass filter from 1 Hz to 40 Hz, segmented (−200 to 900 ms around stimulus onset, baseline: −200 ms to 0 ms), and bad epochs with poor data quality were rejected using EEGLAB. Then, ICA was applied on the remaining segments and resulting ICs weights were written back to the original (i.e. 1000 Hz sampling rate) data. Next, we classified ICs using ICLabel (Pion-Tonachini et al., 2019) and the rejected channels were interpolated. We created epochs of data locked to the cue (As and Bs) and the probe stimuli (Xs and Ys) ranging from −200 ms to 700 ms relative to the respective stimulus, with a baseline period ranging from −200 to 0 ms. In a second analysis (see supplementary results) the epochs ranged from −200 to 3000 ms relative to the onset of the cue and covered both, cue and probe stimuli. Again, the period from −200 to 0 ms served as a baseline. Then we detected and rejected epochs with poor data quality using EEGLAB. On average, 148 ± 58 epochs (out of 960) were rejected in the first and 106 ± 38 epochs (out of 480) were rejected in the second analysis. ICs with a likelihood of less than 30% to represent brain activity and ICS with a likelihood of more than 30% to reflect ocular artifacts were removed from the signal (remaining 18 ± 6 ICs per subject). Subjects with less than 7 remaining ICs were excluded from further analyses (N = 17).

2.4. Classification

We trained linear binary support vector machine classifiers implemented in MATLAB Statistics and Machine Learning Toolbox (MathWorks Inc. MATLAB, 2019a) for both the spatial and temporal EEG signal. The regularization parameter (i.e. lambda) was automatically set to 1/number of observations, and both initial linear coefficients and initial intercept estimates were equal to zero. In general, we classified the data in two ways. We classified the data in the spatial domain to get a temporal representation of decoding accuracy and also in the temporal domain to get a topographical representation of decoding accuracy. For the classification in the spatial domain, we averaged every 5 timepoints without overlap and did the classification for each of these averaged time-points using the data of all electrodes. For the classification in the temporal domain, we did the classification based on 100 ms wide time window with 40% overlap, separately for each electrode. For the latter,

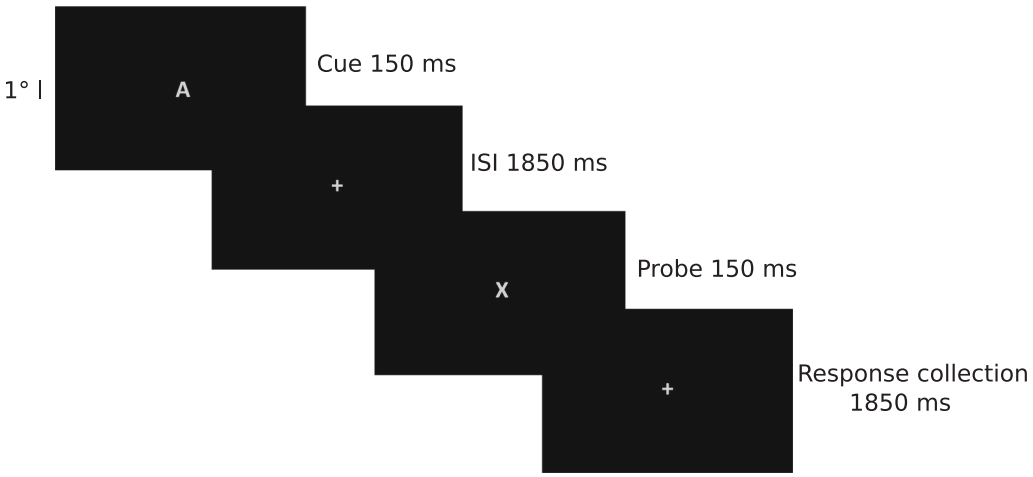

Fig. 1. Stimuli and trials design. Each trial consisted of 150 ms cue, 1850 ms ISI, 150 ms probe, and 1850 ms response collection, successively.

the dimensionality of the data was also reduced to 80% variance (Jolliffe, 2002) using Principal Component Analysis (PCA). For both spatial and temporal classifications, we trained 6 different linear classifiers based on the trials of the following conditions: 1) A vs. B -cue in X-CPT to find the difference between cues with higher probability vs. cues with lower probability of target appearance after them. 2) A vs. B -cue in AX-CPT to figure out information coding difference between target relevant and target irrelevant cues prior to the probe. 3) AX vs. BY -probe in X-CPT and 4) AX vs. BY -probe in AX-CPT to detect the difference between target and nontarget probes. 5) AX-probe in X-CPT vs. AX -probe in AX-CPT to find the effect of implicit vs. explicit target relevant cue on the following target probe. 6) AY-probe in X-CPT vs. AY-probe in AX-CPT to find the effect of implicit vs. explicit target relevant cue on the following nontarget probe. For the second analysis with longer epochs covering cue and probe (presented in the supplementary material), classifications of 1 and 2 are a part of number 3 to 6 classifications. Finally, we predicted AY and BX -probe based on the classification of AX vs. BY -probe for both X-CPT ad AX-CPT. The results are the probability of AY-probe to be classified as AX-probe vs. the probability of the AY-probe to be classified as BY-probe at each time point and for each subject. The same prediction analysis was done for the BX-probe based on AX and BY -probe classifier. We normalized the prediction value by accuracy of AX vs. BY -probe classification. By this way, if the AX and BY -probe classifier was poor in accuracy, it would not have a significant effect on the final prediction results. The normalization was done by multiplying the prediction value with AX vs. BY -probe accuracy in each time point and for each subject. Moreover, as an additional analysis, we grouped the classification results into 3 groups based on the subjects' task performance (i.e. one fifth best, on fifth worst performance and rest of the subjects based on the average commission errors of each subject).

We applied linear classification implementation of MATLAB Statistics and Machine Learning Toolbox (MathWorks Inc. MATLAB, 2019a) with 85% of trials for training and 15% for the test. If there were not equal sample sizes in classification conditions, we used uniform random up-sampling of the smaller sample size with replacement to make the number of trials in the training data equal. The order of the training trials of all conditions were randomized (Bengio, 2012). The number of trials in the test data for both conditions was always 15% of the larger sample size and never up-sampled for any condition.

2.5. Statistical analysis

We applied *t*-tests using MATLAB (MathWorks Inc. MATLAB, 2019a) with the significance level set to 0.05 to compare response times and classification accuracy between conditions. We corrected the p values for multiple comparison of time points and electrodes by means of the false discovery rate method (Benjamini and Hochberg, 1995) implemented in MATLAB (MathWorks Inc. MATLAB, 2019a). For classification, statistical test was done to find the electrodes or time points with significantly higher accuracy than the chance level (i.e. 50%). In all our classifications, we do a classification of two groups with equal number of samples for testing, therefore we consider 50% accuracy as the chance level. The electrodes locations maps are presented only for 100 ms, 200 ms and 380 ms which were the most informative time points to track changes in the pattern of accuracies. However, for the task performance analysis (i.e. Fig. 7) three additional timepoints of 140 ms, 260 ms and 280 ms are also considered. In order to provide an independent statistical comparison of conditions based on task performance (i.e. Fig. 7), we selected target clusters of electrodes, before dividing the data based on the performance conditions (i.e. Fig. 6d for AY-Probe). We targeted for a cluster with highest values of electrodes located over central areas at 100 ms (P1, CP3, CP1, Pz, CPz, P3, CP2, P2, FT10, CP4, POz), as well as, a cluster of electrodes with negative value sited over the prefrontal areas at 380 ms (F3, Fz, F4, FC5, FC1, AF3, AF4, F5, F1, F2, FC3).

3. Results

3.1. Behavioral results

Behavioral results show less ($t(442) = 7.00$, $p < 0.001$) omission errors (only for AX-probe trials) in X-CPT (error: 2.78 ± 5.36%) compared to AX-CPT (error: 4.80 ± 6.80%). Similarly, the rate of commission errors (for AY-probe trials) was lower ($t(442) = 7.51$, $p < 0.001$) in the X-CPT (error: 9.67 ± 15.26%) compared to the AX-CPT (error: 14.82 ± 17.97%). However, response times (for AX-probe trials) were faster ($t(442) = 16.91$, $p < 0.001$) for the AX-CPT (361.19 ± 74.34 ms) compared to the X-CPT (406.82 ± 83.02 ms).

In addition, in the X-CPT, we found significantly faster ($t(442) = 13.11$, $p < 0.001$) responses time after A-cue (406.82 ± 82.02) than B-cue (427.33 ± 85.06). Moreover, the commission error rates after A-cue (error: 9.67 ± 15.26%) was higher ($t(442) = 4.20$, $p < 0.001$) compared to B-cue (error: 8.29 ± 12.55%). However, the omission error rates after B-cue (error 3.17 ± 6.91%) was not significantly higher ($t(442) = 1.53$, $p = 0.13$) than after an A-cue (error 2.78 ± 5.31%).

3.2. Classification: A vs. B −cue in the X-CPT and AX-CPT

We applied linear classification to classify different trial conditions. For X-CPT, we performed both spatial and temporal classifications of A vs B -cue for each subject, and averaged classification results across all subjects. Such classifications will show how the implicit relevance of cue and target probe association is coded in the brain. Spatial classification showed above 50% classification accuracy mainly between 105 ms to 465 ms, with a peak at 165 ms after stimuli onset (Fig. 2a). Fig. 2b shows the temporal classification which highlights an early above-chance accuracy over sensory areas (100 ms after stimulus onset).

For AX-CPT, again we applied both spatial and temporal classifications for each subject and averaged classification results across all subjects. In this way, we tried to find where and when, the activation pattern of cues with explicit association with target vs. nontarget probes are decodable. Spatial classification showed longer above chance classification accuracy than X-CPT (Fig. 2c). This effect started around 100 ms after stimulus onset and lasted to the end of the analyzed time points (i.e. 700 ms after stimulus onset), with peak at 395 ms. Fig. 2d shows the temporal classification of accuracy that, in addition to the early above-chance accuracy over posterior sensory areas, is significantly above chance over posterior visual areas at 200 ms and frontal areas at 380 ms after stimulus onset.

Fig. 2e shows the difference by simple subtracting each subject data in subplot a from the data in subplot c. The difference of A vs. B -cue classification in AX-CPT minus X-CPT is significant from 235 ms after stimulus onset until the end of the analyzed time points with peak at 380 ms. This difference last even after 700 ms (see Supplementary Fig. 1) after stimulus onset.

3.3. Classification: AX vs. BY -probe in the X-CPT and AX-CPT

Fig. 3a shows the spatial classification of AX vs. BY -probe in the X-CPT. This classification detects the difference between most probable target and nontarget probes, where cue is not explicitly, but yet implicitly relevant. Spatial classification showed above 50% classification accuracy starting at 95 ms, with the peak at 425 ms after stimulus onset. Fig. 3b shows the spatiotemporal pattern of classification. The spatiotemporal pattern shows above chance classification over posterior sensory areas at 100 ms that switches to mostly left partial recording sites at 380 ms after the stimulus onset.

For the AX-CPT, classification decoded activation pattern of target vs. nontarget probes, in the case that cue is explicitly relevant. Spatial classification showed earlier above-chance classification accuracy compared to the X-CPT that started around 80 ms after stimulus onset, with peak at 540 ms (Fig. 3c). Fig. 3d shows the temporal classification

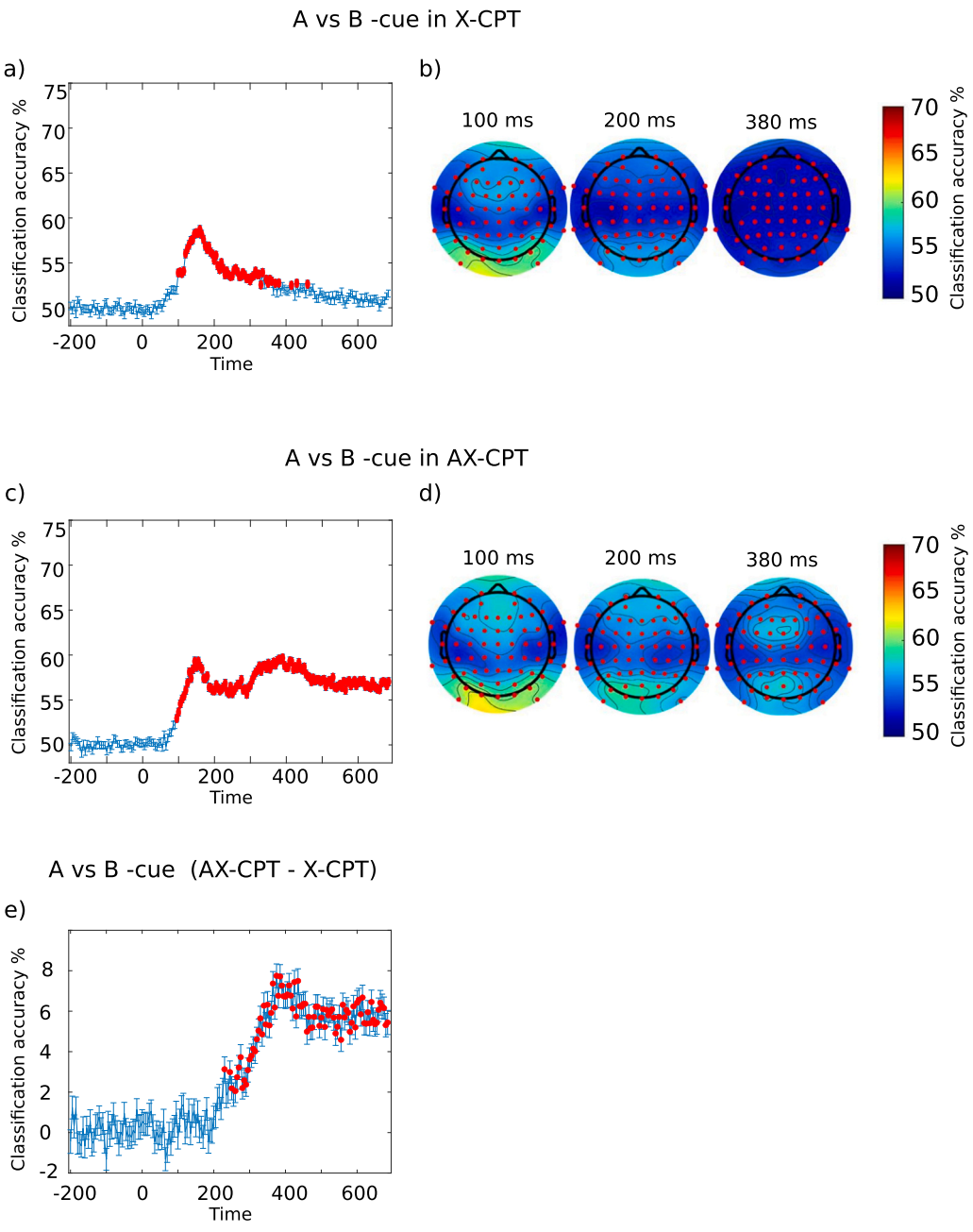

Fig. 2. A vs. B -cues classification for both X-CPT and AX-CPTs. a) Spatial classification of A vs. B -cues in X-CPT. b) Topological map of temporal classification for A vs. B -cues in X-CPT at 100 ms, 200 ms and 380 ms. c) Spatial classification of A vs. B -cues in AX-CPT. d) Topological map of temporal classification for A vs. B -cues in AX-CPT. In the spatial classifications, significant timepoints above chance (i.e. 50%) and in the topological map significant electrodes are highlighted with red color. (For interpretation of the references to color in this figure legend, the reader is referred to the web version of this article.)

of accuracy that is similar to the X-CPT at 100 ms, but shows higher accuracy at 200 ms and 380 ms over parietal areas.

The difference between AX vs. BY -probe classification in AX-CPT minus X-CPT (Fig. 3e) is significant from 100 ms until the end of the analyzed time points, with a peak at 230 ms.

Similar analyses of spatial classification when cue and probe are segmented together are presented in the supplementary materials (Supplementary Fig. 1).

3.4. Classification: AX-probe of the X-CPT vs. AX-probe of the AX-CPT

We classified the AX-probe pattern from the X-CPT vs. the AX-probe pattern from the AX-CPT. With this classification, we aimed to detect the effect of implicit vs. explicit target relevant cue on the following target probe. More specifically, we want to see how proactive effect of an explicit cue would enhance target detection and response programing. Spatial classification showed above 50% classification accuracy starting around 95 ms after stimulus onset, with a peak at 395 ms (Fig. 4a). Temporal classification shows the highest accuracy at 200 ms, with a peak over centro-parietal areas (Fig. 4b).

Spatial classification when cue and probe are segmented together is presented in supplementary materials (Supplementary Fig. 2).

3.5. Classification: AY-probe of the X-CPT vs. AY-probe of the AX-CPT

To see the effect of implicit vs. explicit target relevant cue on the following nontarget probe, we classified AY-probe in X-CPT vs. AY-probe in AX-CPT. This shows, the proactive effect of explicitly relevant cue on both stimuli detection and reactive inhibition of response programing. Fig. 5a shows above 50% spatial classification accuracy starting around 140 ms after stimulus onset, with a peak at 395 ms. Temporal classification shows above-chance accuracy at 380 ms after stimulus onset, with a peak in accuracy over central areas (Fig. 5b).

Spatial classification of the longer segments containing both cue and

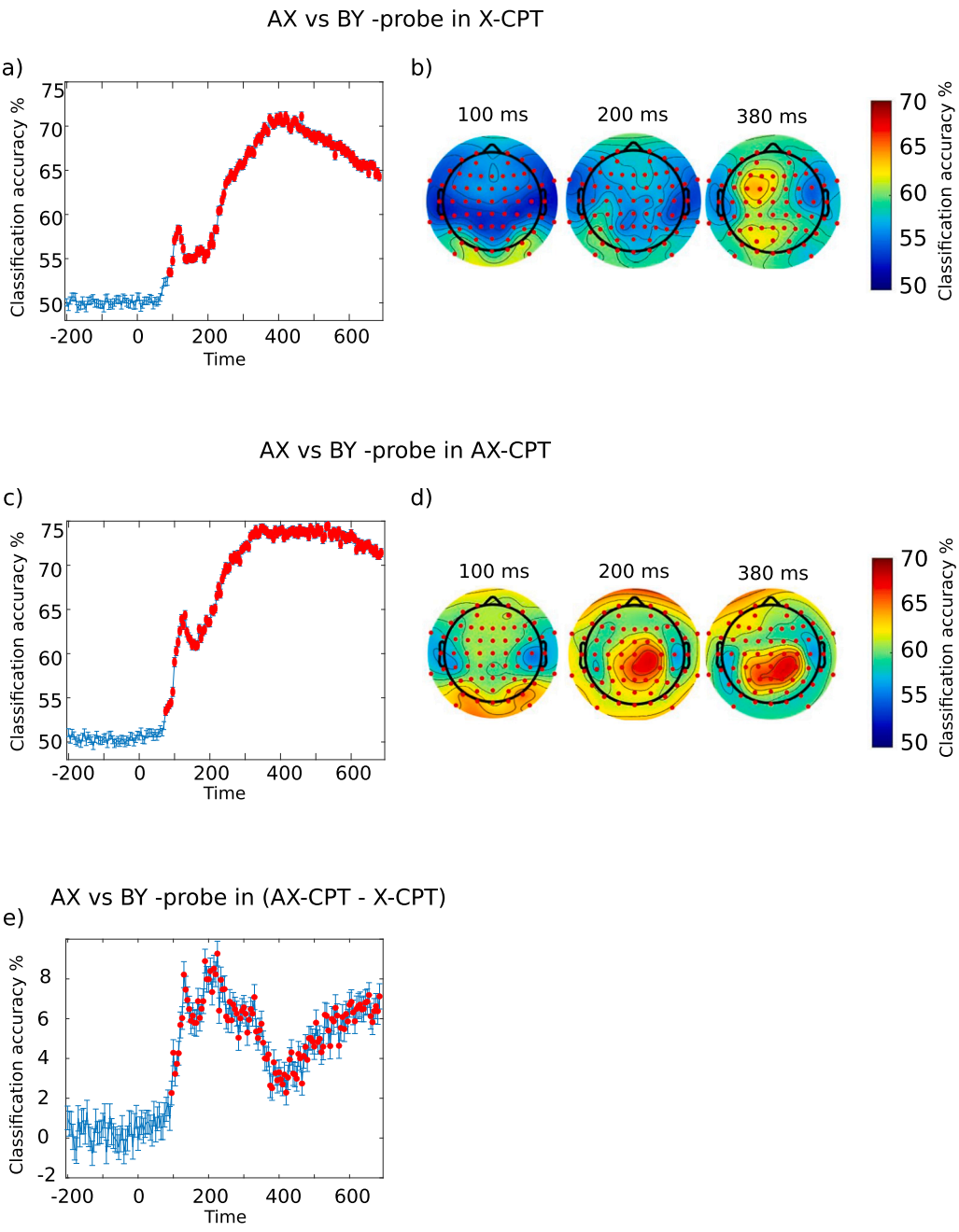

Fig. 3. AX vs. BY -probes classification for both X-CPT and AX-CPTs. a) Spatial classification of AX vs. BY -probes in X-CPT. b) Topological map of temporal classification for AX vs. BY -probes in X-CPT. c) Spatial classification of AX vs. BY -probes in AX-CPT. d) Topological map of temporal classification for AX vs. BY -probes in AX-CPT. In the spatial classifications, significant timepoints above chance and in the topological map significant electrodes are highlighted with red color. (For interpretation of the references to color in this figure legend, the reader is referred to the web version of this article.)

probe is visualized in Supplementary Fig. 3.

3.6. Prediction: AY and BX -probe predictions based on AX vs. BY -probe classification in X-CPT

In the X-CPT, we tried to predict how the AX vs. BY -probe classification model will assign AY or BX -probe to the learned conditions. AX and BY -probe are samples of clear, non-confusing target and nontarget, respectively, with the highest probability to appear in the experiment. This means, by having a classification model about more probable and non-confusing cases of AX and BY -probes, can we get information about how similar AY and BX conflicting probes are to the more probable cases? More specifically, is AY-probe perceived more similar to a non-confusing target (AX-probe) or to a non-confusing nontarget case (BY-probe)? The same question applies to the BX-probe. Spatial prediction showed there is a higher probability that an AY-probe is interpreted as a BY-probe (Fig. 6a). For the AY-probe, the significant time window started at 85 ms, with a peak of similarity to the BY-probe condition at 410 ms after stimulus onset. The BX-probe condition was more similar to the AX-probes and this similarity started at 70 ms and peaked at 400 ms after stimulus presentation. Temporal classification showed comparable results with spatial classification and showed an early similarity over posterior visual areas and a later corresponding effect over left frontal areas (Fig. 6b).

3.7. Prediction: AY and BX -probe predictions based on AX vs. BY -probe classification in AX-CPT

A similar prediction analysis was done for the AX-CPT. Spatial prediction showed somehow mixed similarity of the AY-probe condition to both the AX and BY -probes (Fig. 6c). AY-probe was similar AX-probe mainly at 145 ms to 255 ms, and later at 330 ms to 345 ms after

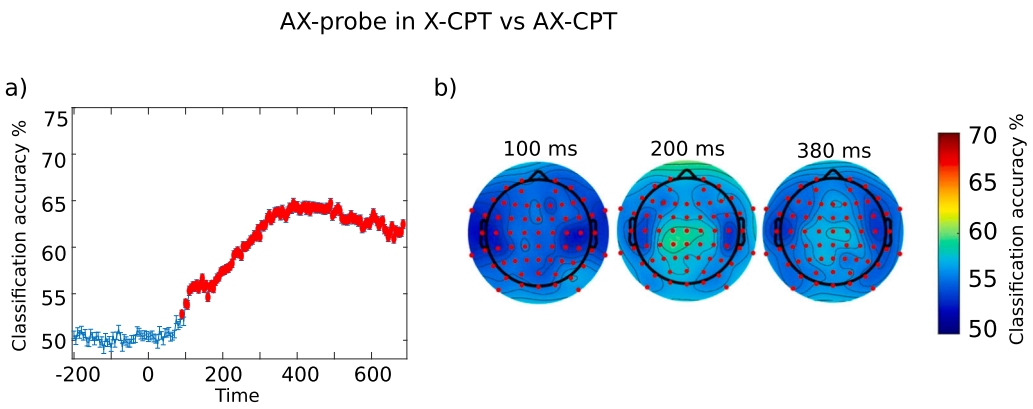

Fig. 4. AX -probes classification in X-CPT vs. AX-CPTs. a) Spatial classification. b) Topological map of the temporal classification at 100 ms, 200 ms, and 380 ms. In the spatial classifications, significant timepoints above chance and in the topological map significant electrodes are highlighted with red color. (For interpretation of the references to color in this figure legend, the reader is referred to the web version of this article.)

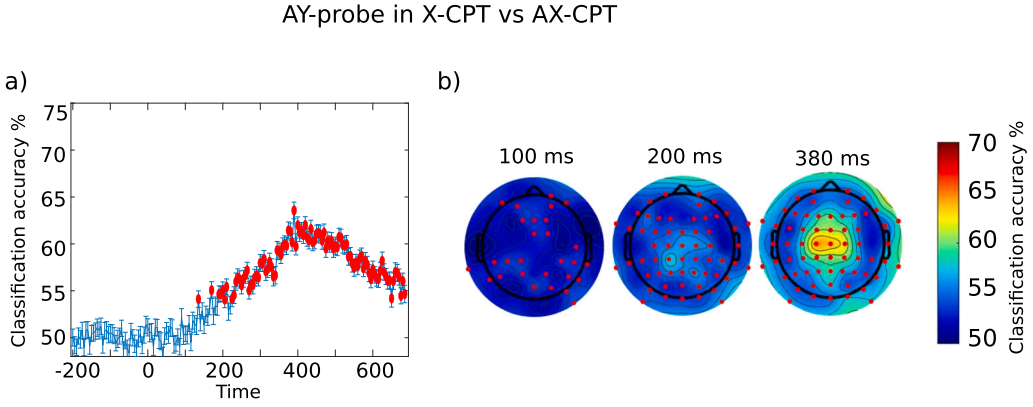

Fig. 5. AY -probes classification in X-CPT vs. AX-CPTs. a) Spatial classification. b) Topological map of temporal classification at 100 ms, 200 ms, and 380 ms. In the spatial classifications, significant timepoint above chance and in the topological map significant electrodes are highlighted with red color. (For interpretation of the references to color in this figure legend, the reader is referred to the web version of this article.)

stimuli onset, with a peak of similarity at 335 ms. However, at 105 ms to 125 ms after stimulus onset, the AY-probe condition was most similar to the BY-probes, with a peak at 115 ms. As expected, temporal classification showed a similarity to the BY-probe condition mostly over visual areas at around 100 ms after stimulus onset (Fig. 6d). The BX-probes were more similar to the AX-probes mainly between 85 and 130 ms, with a peak at 110 ms. However, at later stages, the BX-probes showed more similarity to the nontarget BY-probes, with a start at 115 ms and a peak at 500 ms after stimulus onset.

To control whether the subjects' task performance is linked to differences in patterns of the prediction analyses, we split the subjects into 3 groups based on their commission error rate. The one fifth of the subjects with least and one fifth of the subjects with most commission errors were analyzed separately. Fig. 7a and b show the prediction for the spatiotemporal pattern of the AY-probe, based on correct trials (comparable to Fig. 6d) for 20% of subjects with the least (a) and 20% of subjects with the most commission errors (b), respectively. At 260 ms and 280 ms after stimulus onset, despite the difference in the visual pattern, the similarity to nontarget BY-probe was not significantly different between these two conditions, for the independently pre-selected cluster over the prefrontal area (based on negative cluster in Fig. 6d, see Methods). Moreover, for 20% of the subjects with the worst task performance (i.e. highest commission error), we further predicted the spatiotemporal pattern of AY-probe for incorrect trials (Fig. 7c). We compared the correct (a) and incorrect (c) AY-trials for the subject with the lowest and highest commission errors. Based on the independent pre-selection cluster of electrodes over central areas (highest value cluster in Fig. 6d, see Methods), similarity of AY-probe to AX-probe was larger ($t(174) = 2.72$, $p < 0.004$) for incorrect trials of the subjects with highest commission error (Fig. 7c) compared to correct trials of the subjects with lowest commission error (Fig. 7a) at 140 ms. In addition, at 260 ms, for pre-selected cluster of electrodes over prefrontal area (based on negative value cluster in Fig. 6d), similarity of AY-probe to BY-probe was larger ($t(174) = 1.91$, $p < 0.03$) for correct trials of the subjects with lowest commission error (Fig. 7a) compared to incorrect trials of the subjects with highest commission errors (Fig. 7c). To further test the robustness of our results to percentile selection, we repeated the performance effect analysis for division of the subjects into two groups. We median split the subjects based on their performances, and our analysis lead to comparable results with the 20% extreme divisions.

4. Discussion

In the present study, the participants performed in versions of the X-CPT and AX-CPT neurocognitive tasks with fixed global but varying local probabilities of cue and probe appearances. We collected behavioral and EEG data from a large sample size of healthy subjects (N = 460) to learn about reactive and proactive cognitive control mechanisms involved in these tasks (Lesh et al., 2013; Polizzotto et al., 2018; Mäki-Marttunen et al., 2019; Gonthier et al., 2016). Our versions of the X-CPTs and AX-CPT tasks were designed to require various cognitive processes related to attention and response preparation (Lewis et al., 2017; Smid et al., 2006). In the task versions deployed, the X-CPT is a sustained attention and implicit transient response preparation task and

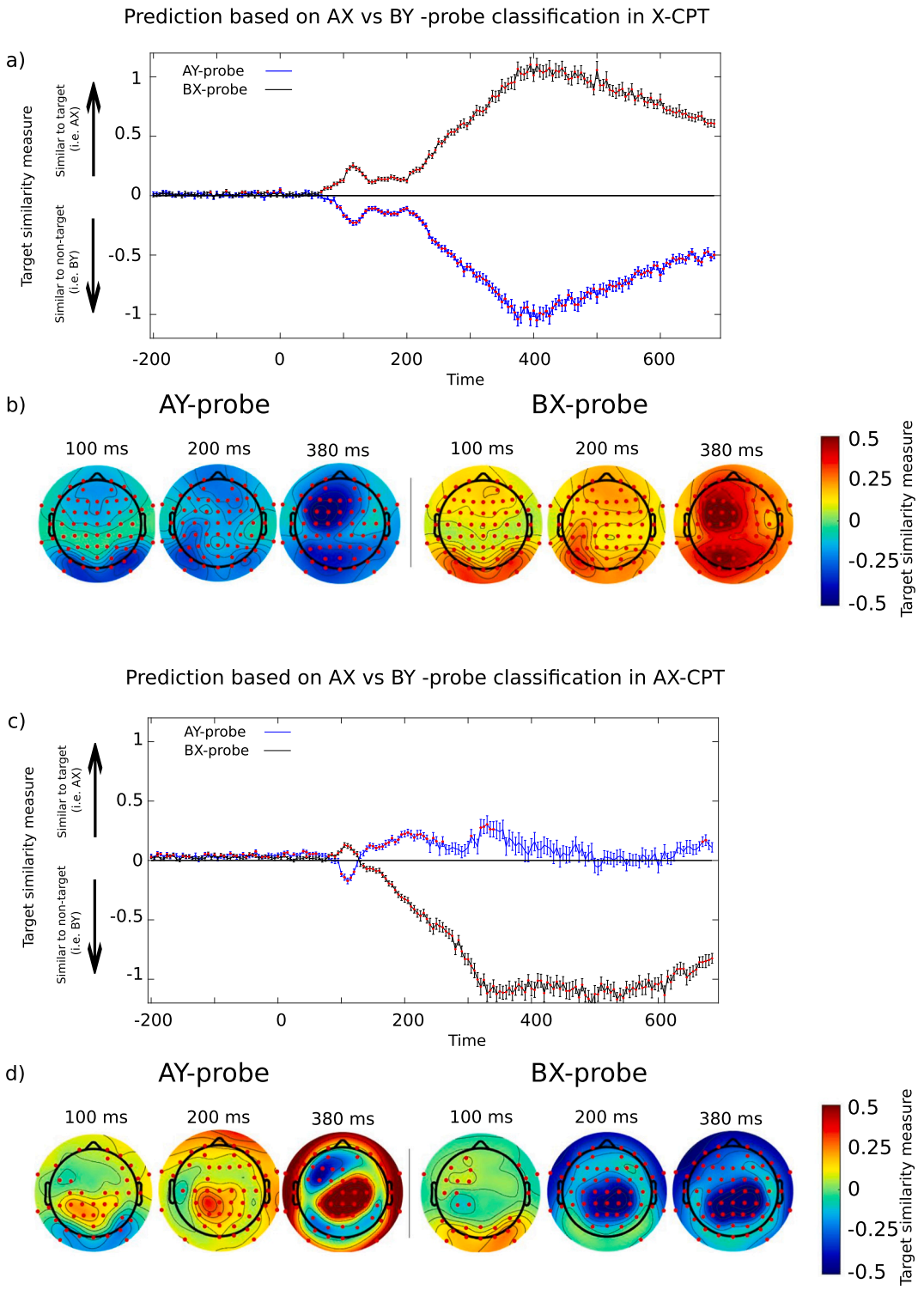

Fig. 6. Prediction of AY and BX -probes based on classification of AX-probe vs. BY-probe. a) Spatial perdition of AY and BX -probe in X-CPT. b) Spatiotemporal prediction of AY and BX -probe in X-CPT. c) Spatial perdition of AY and BX -probe in AX-CPT. d) Spatiotemporal pattern of AY and BX -probe predictions in AX-CPT. In the spatial prediction, significant timepoints above zero and in the topological map significant electrodes are highlighted with red color. (For interpretation of the references to color in this figure legend, the reader is referred to the web version of this article.)

the AX-CPT is a transient attention and both implicit and explicit response preparation task (Smid et al., 2006). Previous research on CPT variations concentrates on how sustained and transient attention and response preparation are reflected in behavioral performance as well as in various ERP components (Karamacoska et al., 2019; Wascher et al., 2020; Lau-Zhu et al., 2019; Smid et al., 2006). Our aim was to utilize artificial intelligence techniques to expand our current knowledge about the cognitive processes involved. However, in order to interpret the results properly, it is important that the electrophysiological data are comparable to previous studies deploying a similar design. Fig. 8 depicts the ERP wave-forms for the electrodes FCz and Pz for X and Y -probes in both X-CPT and AX-CPT. Regarding the ERPs, recent findings could be

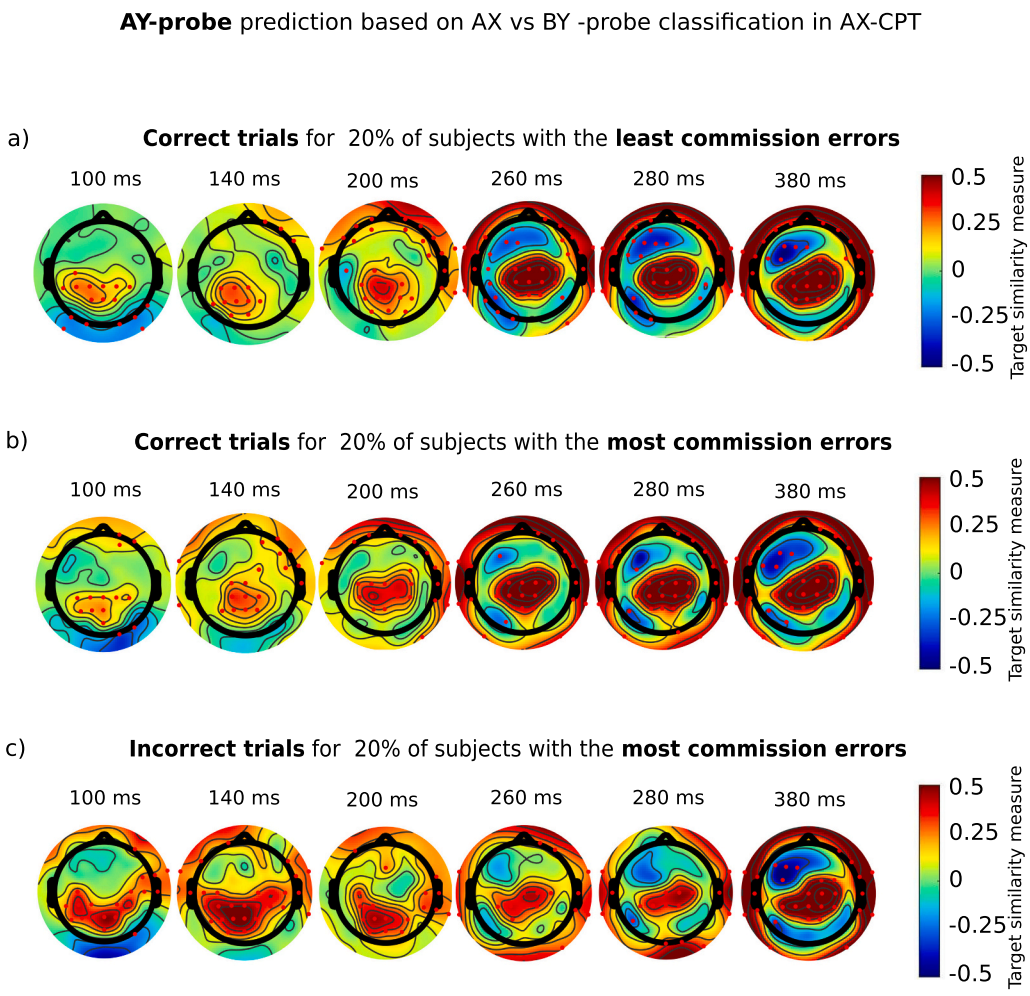

Fig. 7. Split of the subjects AY-probe prediction based on their overall commission error rate in AX-CPT and individual trials performances. The temporal pattern of AY-probe prediction based on the correct trials (comparable to Fig. 6d) for 20% of the subjects with least (a) and 20% of the subjects with most (b) commission errors. c) The temporal pattern of AY-probe prediction based on incorrect trials for 20% of the subjects with the most commission errors. The temporal patterns are presented at 100 ms, 140 ms, 200 ms, 260ms, 280 ms and 380 ms. All the predictions are based on AX vs BY -probe classifier trained on the correct trials. Significant electrodes with values higher than zero highlighted with red color. (For interpretation of the references to color in this figure legend, the reader is referred to the web version of this article.)

replicated (cf. Wascher et al., 2020).

Our results show that A and B -cues could be classified (Fig. 2) early in both the X-CPT and AX-CPT versions. These classification results could at least partially be an evidence for implicit statistical information learning carried by the cues. In this way, in the X-CPT we could see significant decodability of the neural activation patterns of A vs. B -cue (Fig. 2a–b) over the occipital areas. Such finding is also in line with our behavior results which shows faster responses time after A than B -cue, higher commission errors after A vs B -cue, and higher omission errors after B vs. A- cues in X-CPT. Moreover, our behavioral results show that despite less commission and omission errors, the response time was slower in the X-CPT compared to the AX-CPT (Smid et al., 2006; Wascher et al., 2020; Dias et al., 2003). Our classification results show that when the cue also explicitly defines the target stimulus (AX-CPT), the detectability of brain states starts immediately after the visual processing of the cues (Fig. 2) and even lasts during the inter-stimulus intervals (Supplementary Fig. 1). This detectability is not evident when the cue is not explicitly relevant for defining the target stimulus (X-CPT). Such a clear activation pattern classification in the AX-CPT which is mainly observed over frontal areas after cue presentation and before probe onset (Fig. 2) could be associated with very early proactive response programming (Richmond et al., 2015; Redick, 2014). In line, previous ERP findings report CNV reflecting cognitive or motor preparation (Ulrich et al., 1998; Brunia, 1993) after the target-related A-cue, but not the B-cue in AX-CPT (Smid et al., 2006).

In addition, in both the X-CPT and AX-CPT, the most probable target (AX-probe) and nontarget (BY-probe) probes were decodable over posterior areas early after stimulus presentation (Fig. 3). However, this decodability was larger in the AX-CPT and continued until response generation (200 ms) over central and partial sites. Around the time of response generation (380 ms), again for both the X-CPT and AX-CPT, the two probes were decodable over the left frontal and parietal cortex, respectively, albeit with larger values in AX-CPT. At 380 ms, the X-CPT showed significant detectability over the lateral frontal cortex, as well. In general, target vs. nontarget detectability seems to be mainly different in the X-CPT compared to the AX-CPT from 150 ms to 350 ms after stimulus onset (Fig. 3e), which could reflect a difference in response preparation between these two tasks. However, the detection of AX vs. BY -probes differed significantly between the two tasks already around 100 ms after stimulus onset. We hypothesize that such an early difference in activation patterns in response to the probe-stimuli could be associated with different levels preparation provided by the cue (Battistoni et al., 2017) in sustained vs. transient attention conditions. In addition, previous studies (Smid et al., 2006; Wascher et al., 2020; Dias et al., 2003) suggested that transient response preparation led to faster task performance. However, in our design, both the X-CPT and AX-CPT request for transient response preparation. Therefore, the faster response times in the AX-CPT compared to the X-CPT could originate from an explicit transient response preparation in the AX-CPT. To directly compare the effect of implicit and explicit transient response preparation on task performance, another classical X-CPT study with similar local and global target probability is needed. Moreover, we could see the classification difference for target and nontarget activation patterns between the X-CPT and AX-CPT even at a time after the average response time (Fig. 3e). This might be due to individual difference in response time or might reflect difference in preparation for the next cue

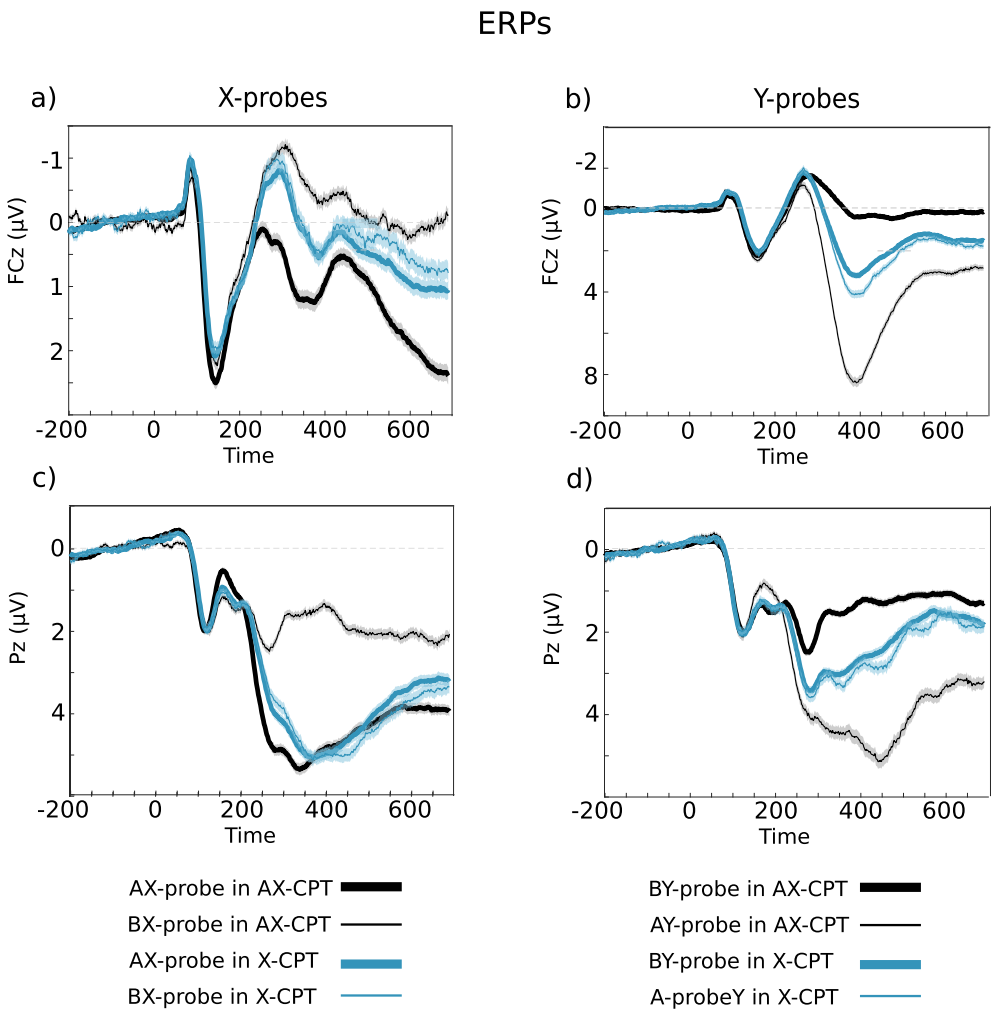

Fig. 8. Average ERPs for two selected electrodes across all subjects in X-CPT and AX-CPT. a) ERPs of FCz electrode for X-probes (i.e. AX-probe and BX-probe), b) ERPs of FCz electrode for Y-probes (i.e. BY-probe and AY-probe), c) ERPs of Pz electrode for X-probes, and d) ERPs of Pz electrode for Y-probes. The shades show standard error of means. (For interpretation of the references to color in this figure legend, the reader is referred to the web version of this article.)

detection when the cue is task relevant vs. when it is not task relevant.

Although the AX-probe was a probable target in both X-CPT and AX-CPTs, it still produced different activation patterns for the two tasks which were detectable mainly around time periods that are related to higher-level attentional processing and response preparation (200 ms) and over centro-parietal cortex (Fig. 4). Also, the AY-probes nontarget in both tasks created different EEG patterns at 200 ms, but mainly around a time window that might be to higher extend related to response generation (380 ms after stimulus onset) over central recording sites (Fig. 5). Such a higher detectability of response patter could be due to response preparation and action planning in AY-probes in AX-CPT. Principally, the X-CPT requests for a sustained attention and probably needs less working memory load for task control than the AX-CPT (Braver, 2012). In addition, such a sustained attention is associated with less commission and omission errors in X-CPT compared to AX-CPT (Smid et al., 2006; Wascher et al., 2020; Borgaro et al., 2003; Coons et al., 1981). Findings from ERP studies indicate that this higher target detection performance originates from better visual selective processing which is reflected in larger SN amplitude in the X-CPT compared to the AX-CPT (Smid et al., 2006; Eimer, 1997; Smid et al., 1999). Our classification results confirm that, even at very early stages of processing (starting from 95 ms after stimuli onset), the AX-probe generates different activation patterns in the X-CPT compared to the AX-CPT. From temporal classification view this detectability around 100 ms is mainly over the occipital areas (Fig. 4). Similarly, the AY-probe provoked a detectable pattern in the X-CPT compared to the AX-CPT, starting already at 140 ms after stimulus onset (Fig. 5). In these cases, the cue before the two probes are probable, and carry statistical information that is directly linked to target expectation. However, the difference comes from different level of proactive readiness for potential target due to the explicit instructions in the two X-CPT vs. AX-CPT.

Furthermore, it was possible to predict the EEG response pattern for rare probes (i.e. AY-probes and BX-probes) based on what has been learned from probable AX and BY -probes (Fig. 6). As anticipated for the X-CPT, AY-probes generated a pattern similar to BY-probes, and BX-probes generated a pattern similar to AX-probes, as the cues were explicitly task-irrelevant. This similarity was observable initially over occipital cortex and later over the left frontal cortex. However, in the AX-CPT, AY-probes showed a different similarity pattern than in the X-CPT. Although AY-probes generated a similar pattern to BY- probes at 100 ms over posterior areas, they showed a strong similarity in EEG patterns to AX-probes over central and parietal recording sites. Concurrently, at 380 ms AY-probe generated a similar pattern to BY-probe over the frontal cortex. In the X-CPT, as the cue was not explicitly but only implicitly relevant, the AY-Probe was detected as a BY-probe, and the BX-probe was detected as an AX-probe. In fact, the implicit information coming from the local statistics of the cue did not seem to affect or make difference between the probable vs. non-probable probes. However, in the AX-CPT, where the cue was both implicitly and explicitly relevant, the AY-probe was detected as a BY- probe over

the occipital areas at 100 ms following stimulus presentation. A task relevant A-cue did not seem to make a delay in this detection compared to the detection of BX-probes. But later, due to response expectation based on the explicit cue, the AY-probes were more similar to the AX-probes, specifically before response generation. Our temporal classification showed similar confusion mainly focused over parietal areas (Fig. 6d). In addition, the AY-probes featured a pattern similarity to the BY-probes over the frontal cortex. This might be related to the inhibition of response generation in this nontarget condition. Such a finding might indicate the presence of a higher order feedback control system involved in the processes associated with violation of expectations.

To better investigate if the AY-probes pattern similarity to BY-probes over the frontal cortex might be related to response inhibition in the AX-CPT, we further grouped our analysis based on the subjects' task performance. We compared three conditions including correct trials of subjects with least commission errors (Fig. 7a), correct trials of subjects with most commission errors (Fig. 7b), and incorrect trials of subjects with most commission errors (Fig. 7c). In this way, the similarity of the AY-probe to the BY-probe was higher for the pre-selected cluster of electrodes over the pre-frontal area in the correct trials of subjects with overall least commission errors vs. incorrect trials of the subjects with most commission errors at 260 ms (Fig. 7a vs. c). Based on comparison of overall patterns in these three groups (Fig. 7a–c), we hypothesize, that higher similarity to BY-probe is linked to a more pronounced inhibitory feedback control that suppresses response preparation in case of confusing cue in the subjects with lower vs. higher commission errors. Besides, for the pre-selected cluster over the parietal areas, early (i.e. 140 ms after stimuli onset) similarity of AY-probe to AX-probe was higher for incorrect trials of subjects with most commission errors than the correct trials of subjects with least commission errors. This result intimate that not only a top down control, but also an initially higher tendency of response preparation is an influential factor on the task performance.

Our current study has some limitation as well. First, considering the early decoding accuracy, there is a possibility that other underlying processes, such as lower-level differences in perception also play role in the decoding of activation patterns. In future directions, a design including more than one non-target cue has the potential to better compare the effect of attention difference vs. perceptual processing. In this way, we expect that the difference between decoding of target-relevant vs. non-target cues and decoding of two non-target cues mostly be related to attention differences compared to perceptual processing. Second, in our design, AX-CPT was performed before X-CPT. Therefore, AX-CPT might have some aftereffect on X-CPT. For example, the implicit statistical information of cue-probe associations which are learned during AX-CPT, might be present from beginning of X-CPT. However, we do not expect such an aftereffect have a large impact on our results. Third, we used SVM for our classifications. SVM is a robust classification method when the data has several dimensions and minimum knowledge is available about the nature of the data. However, SVM is computationally demanding, it is not easy to interpret the model, and selection of the kernel function is not often easy to be optimized (Auria and Moro, 2008; Bhavsar and Panchal, 2012).

To conclude, with the new perspective based on machine learning methods, we tried to characterize the CPT related cognitive control functions at each stage of information processing. Our MVPA revealed both spatial and temporal properties of sustained vs. transient attention and response preparation. In addition, our findings could suggest the presence of a higher order feedback inhibitory control that regulates initial proactive response preparation. Such an inhibitory mechanism seems to affect both overall task performance as well as performance of each trial. Moreover, the balance between the initial proactive response preparation and later reactive inhibitory mechanisms seems to play a key role in the task outcome. Therefore, our more complete map of cognitive functions involved in the CPT has the potential to provide EEG based markers in future clinical applications (Braver et al., 2005; Barch et al., 2001; MacDonald and Carter, 2003; Slobodin, 2020).

Acknowledgments

We would like to thank people who organized and collected data for the Dortmund Vital Study.

Appendix A. Supplementary data

Supplementary data to this article can be found online at https://doi.org/10.1016/j.ijpsycho.2021.06.012.

References

Alizadeh, Sarah, Jamalabadi, Hamidreza, Schönauer, Monika, Leibold, Christian, Gais, Steffen, 2017. Decoding cognitive concepts from neuroimaging data using multivariate pattern analysis. NeuroImage 159, 449–458. https://doi.org/10.1016/j.neuroimage.2017.07.058.

Auria, Laura., Moro, Rouslan A., 2008. Support Vector Machines (SVM) as a Technique for Solvency Analysis.

Barch, D.M., Carter, C.S., Braver, T.S., Sabb, F.W., MacDonald, A., Noll, D.C., Cohen, J. D., 2001. Selective deficits in prefrontal cortex function in medication-naive patients with schizophrenia. Arch. Gen. Psychiatry 58 (3), 280–288. https://doi.org/10.1001/archpsyc.58.3.280.

Battistoni, Elisa, Stein, Timo, Peelen, Marius V., 2017. Preparatory attention in visual cortex. Ann. N. Y. Acad. Sci. 1396 (1), 92–107. https://doi.org/10.1111/nyas.13320.

Bengio, Yoshua, 2012. Practical recommendations for gradient-based training of deep architectures. Available online at. https://arxiv.org/abs/1206.5533.

Benjamini, Yoav, Hochberg, Yosef, 1995. Controlling the False Discovery Rate: A Practical and Powerful Approach to Multiple Testing, pp. 289–300.

Bhavsar, Himani, Panchal, Mahesh H., 2012. A Review on Support Vector Machine for Data Classification.

Borgaro, Susan, Pogge, David L., DeLuca, Victoria A., Bilginer, Lale, Stokes, John, Harvey, Philip D., 2003. Convergence of different versions of the continuous performance test: clinical and scientific implications. J. Clin. Exp. Neuropsychol. 25 (2), 283–292. https://doi.org/10.1076/jcen.25.2.283.13646.

Braver, Todd S., 2012. The variable nature of cognitive control: a dual mechanisms framework. Trends Cogn. Sci. 16 (2), 106–113. https://doi.org/10.1016/j.tics.2011.12.010.

Braver, Todd S., Satpute, Ajay B., Rush, Beth K., Racine, Caroline A., Barch, Deanna M., 2005. Context processing and context maintenance in healthy aging and early stage dementia of the Alzheimer's type. Psychol. Aging 20 (1), 33–46. https://doi.org/10.1037/0882-7974.20.1.33.

Braver, Todd S., Paxton, Jessica L., Locke, Hannah S., Barch, Deanna M., 2009. Flexible neural mechanisms of cognitive control within human prefrontal cortex. In: Proceedings of the National Academy of Sciences of the United States of America, pp. 7351–7356. https://doi.org/10.1073/pnas.0808187106.

Brunia, C.H., 1993. Waiting in readiness: gating in attention and motor preparation. Psychophysiology 30 (4), 327–339. https://doi.org/10.1111/j.1469-8986.1993.tb02054.x.

Cichy, Radoslaw Martin, Pantazis, Dimitrios, 2017. Multivariate pattern analysis of MEG and EEG: a comparison of representational structure in time and space. NeuroImage 158, 441–454. https://doi.org/10.1016/j.neuroimage.2017.07.023.

Cohen, J.D., Servan-Schreiber, D., 1992. Context, cortex, and dopamine: a connectionist approach to behavior and biology in schizophrenia. Psychol. Rev. 99 (1), 45–77. https://doi.org/10.1037/0033-295x.99.1.45.

Cohen, J.D., Barch, D.M., Carter, C., Servan-Schreiber, D., 1999. Context-processing deficits in schizophrenia: converging evidence from three theoretically motivated cognitive tasks. J. Abnorm. Psychol. 108 (1), 120–133. https://doi.org/10.1037//0021-843x.108.1.120.

Coons, H.W., Peloquin, L.J., Klorman, R., Bauer, L.O., Ryan, R.M., Perlmutter, R.A., Salzman, L.F., 1981. Effect of methylphenidate on young adult's vigilance and event-related potentials. Electroencephalogr. Clin. Neurophysiol. 51 (4), 373–387. https://doi.org/10.1016/0013-4694(81)90101-2.

Cristianini, Nello, Shawe-Taylor, John, 2000. An Introduction to Support Vector Machines. And Other Kernel-based Learning Methods/Nello Cristianini and John Shawe-Taylor. Cambridge University Press, New York.

Delorme, Arnaud, Makeig, Scott, 2004. EEGLAB: an open source toolbox for analysis of single-trial EEG dynamics including independent component analysis. J. Neurosci. Methods 134 (1), 9–21. https://doi.org/10.1016/j.jneumeth.2003.10.009.

Dhar, Monica, Been, Pieter H., Minderaa, Ruud B., Althaus, Monika, 2010. Information processing differences and similarities in adults with dyslexia and adults with Attention Deficit Hyperactivity Disorder during a Continuous Performance Test: a study of cortical potentials. Neuropsychologia 48 (10), 3045–3056. https://doi.org/10.1016/j.neuropsychologia.2010.06.014.

Dias, Elisa C., Foxe, John J., Javitt, Daniel C., 2003. Changing plans: a high density electrical mapping study of cortical control. Cereb. Cortex (New York, N.Y. : 1991) 13 (7), 701–715. https://doi.org/10.1093/cercor/13.7.701.

Eimer, M., 1996. ERP modulations indicate the selective processing of visual stimuli as a result of transient and sustained spatial attention. Psychophysiology 33 (1), 13–21. https://doi.org/10.1111/j.1469-8986.1996.tb02104.x.

Eimer, M., 1997. An event-related potential (ERP) study of transient and sustained visual attention to color and form. Biol. Psychol. 44 (3), 143–160. https://doi.org/10.1016/s0301-0511(96)05217-9.

Elvevåg, B., Weinberger, D.R., Suter, J.C., Goldberg, T.E., 2000. Continuous performance test and schizophrenia: a test of stimulus-response compatibility, working memory, response readiness, or none of the above? Am. J. Psychiatry 157 (5), 772–780. https://doi.org/10.1176/appi.ajp.157.5.772.

Fahrenfort, Johannes J., van Leeuwen, Jonathan, Olivers, Christian N.L., Hogendoorn, Hinze, 2017. Perceptual integration without conscious access. Proc. Natl. Acad. Sci. U. S. A. 114 (14), 3744–3749. https://doi.org/10.1073/pnas.1617268114.

Fahrenfort, Johannes J., van Driel, Joram, van Gaal, Simon, Olivers, Christian N.L., 2018. From ERPs to MVPA using the Amsterdam decoding and modeling toolbox (ADAM). Front. Neurosci. 12, 368. https://doi.org/10.3389/fnins.2018.00368.

Fallgatter, A.J., 2001. Electrophysiology of the prefrontal cortex in healthy controls and schizophrenic patients: a review. J. Neural Transm. (Vienna, Austria : 1996) 108 (6), 679–694. https://doi.org/10.1007/s007020170045.

Gonthier, Corentin, Macnamara, Brooke N., Chow, Michael, Conway, Andrew R.A., Braver, Todd S., 2016. Inducing proactive control shifts in the AX-CPT. Front. Psychol. 7, 1822. https://doi.org/10.3389/fpsyg.2016.01822.

Hackley, S.A., Schäffer, R., Miller, J., 1990. Preparation for Donders' type B and C reaction tasks. Acta Psychol. 74 (1), 15–33. https://doi.org/10.1016/0001-6918(90)90032-b.

Halperin, J.M., 1991. The clinical assessment of attention. Int. J. Neurosci. 58 (3–4), 171–182. https://doi.org/10.3109/00207459108985433.

Jolliffe, I.T., 2002. Principal Component Analysis, 2nd ed. Springer (Springer series in statistics), New York, London.

Karamacoska, Diana, Barry, Robert J., Blasio, Frances M. de, Steiner, Genevieve Z., 2019. EEG-ERP dynamics in a visual continuous performance test. Int. J. Psychophysiol. 146, 249–260. https://doi.org/10.1016/j.ijpsycho.2019.08.013.

Lau-Zhu, Alex, Tye, Charlotte, Rijsdijk, Frühling, McLoughlin, Grainne, 2019. No evidence of associations between ADHD and event-related brain potentials from a continuous performance task in a population-based sample of adolescent twins. PLoS One 14 (10), e0223460. https://doi.org/10.1371/journal.pone.0223460.

Lesh, Tyler A., Westphal, Andrew J., Niendam, Tara A., Yoon, Jong H., Minzenberg, Michael J., Ragland, J. Daniel, et al., 2013. Proactive and reactive cognitive control and dorsolateral prefrontal cortex dysfunction in first episode schizophrenia. Neuroimage Clin. 2, 590–599. https://doi.org/10.1016/j.nicl.2013.04.010.

Leuthold, H., Sommer, W., Ulrich, R., 1996. Partial advance information and response preparation: inferences from the lateralized readiness potential. J. Exp. Psychol. Gen. 125 (3), 307–323. https://doi.org/10.1037//0096-3445.125.3.307.

Lewis, Frances C., Reeve, Robert A., Kelly, Simon P., Johnson, Katherine A., 2017. Sustained attention to a predictable, unengaging Go/No-Go task shows ongoing development between 6 and 11 years. Atten. Percept. Psychophys. 79 (6), 1726–1741. https://doi.org/10.3758/s13414-017-1351-4.

Lotte, F., Bougrain, L., Cichocki, A., Clerc, M., Congedo, M., Rakotomamonjy, A., Yger, F., 2018. A review of classification algorithms for EEG-based brain-computer interfaces: a 10 year update. J. Neural Eng. 15 (3), 31005. https://doi.org/10.1088/1741-2552/aab2f2.

Luck, Steven J., 2014. An Introduction to the Event-related Potential Technique, second edition. The MIT Press, Cambridge.

MacDonald, Angus W., Carter, Cameron S., 2003. Event-related FMRI study of context processing in dorsolateral prefrontal cortex of patients with schizophrenia. J. Abnorm. Psychol. 112 (4), 689–697. https://doi.org/10.1037/0021-843X.112.4.689.

Mäki-Marttunen, V., Hagen, T., Espeseth, T., 2019. Proactive and reactive modes of cognitive control can operate independently and simultaneously. Acta Psychol. 199, 102891. https://doi.org/10.1016/j.actpsy.2019.102891.

Nichols, Shana L., Waschbusch, Daniel A., 2004. A review of the validity of laboratory cognitive tasks used to assess symptoms of ADHD. Child Psychiatry Hum. Dev. 34 (4), 297–315. https://doi.org/10.1023/B:CHUD.0000020681.06865.97.

Ornitz, E.M., Gehricke, J.G., Russell, A.T., Pynoos, R., Siddarth, P., 2001. Modulation of startle and the startle-elicited P300 by the conditions of the cued continuous performance task in school-age boys. Clin. Neurophysiol. 112 (12), 2209–2223. https://doi.org/10.1016/s1388-2457(01)00686-1.

Pion-Tonachini, Luca, Kreutz-Delgado, Ken, Makeig, Scott, 2019. ICLabel: an automated electroencephalographic independent component classifier, dataset, and website. NeuroImage 198, 181–197. https://doi.org/10.1016/j.neuroimage.2019.05.026.

Polizzotto, Nicola Riccardo, Hill-Jarrett, Tanisha, Walker, Christopher, Cho, Raymond Y., 2018. Normal development of context processing using the AXCPT paradigm. PLoS One 13 (5), e0197812. https://doi.org/10.1371/journal.pone.0197812.

Redick, Thomas S., 2014. Cognitive control in context: working memory capacity and proactive control. Acta Psychol. 145, 1–9. https://doi.org/10.1016/j.actpsy.2013.10.010.

Riccio, Cynthia A., Reynolds, Cecil R., Lowe, Patricia, Moore, Jennifer J., 2002. The continuous performance test: a window on the neural substrates for attention? Arch. Clin. Neuropsychol. 17 (3), 235–272.

Richmond, Lauren L., Redick, Thomas S., Braver, Todd S., 2015. Remembering to prepare: the benefits (and costs) of high working memory capacity. J. Exp. Psychol. Learn. Mem. Cogn. 41 (6), 1764–1777. https://doi.org/10.1037/xlm0000122.

Rosvold, K.E., Mirsky, A.F., Sarason, I., Bransome, E.D., Beck, L.H., 1956. A continuous performance test of brain damage. J. Consult. Psychol. 20 (5), 343–350. https://doi.org/10.1037/h0043220.

Servan-Schreiber, D., Cohen, J.D., Steingard, S., 1996. Schizophrenic deficits in the processing of context. A test of a theoretical model. Arch. Gen. Psychiatry 53 (12), 1105–1112. https://doi.org/10.1001/archpsyc.1996.01830120037008.

Slobodin, Ortal, 2020. The utility of the CPT in the diagnosis of ADHD in individuals with substance abuse: a systematic review. Eur. Addict. Res. 26 (4–5), 283–294. https://doi.org/10.1159/000508041.

Smid, H.G., Jakob, A., Heinze, H.J., 1999. An event-related brain potential study of visual selective attention to conjunctions of color and shape. Psychophysiology 36 (2), 264–279. https://doi.org/10.1017/s0048577299971135.

Smid, H.G., Fiedler, R., Heinze, H.J., 2000. An electrophysiological study of the insertion of overt response choice. J. Exp. Psychol. Hum. Percept. Perform. 26 (3), 1053–1071. https://doi.org/10.1037//0096-1523.26.3.1053.

Smid, H.G.O.M., de Witte, M.R., Homminga, I., van den Bosch, R.J., 2006. Sustained and transient attention in the continuous performance task. J. Clin. Exp. Neuropsychol. 28 (6), 859–883. https://doi.org/10.1080/13803390591001025.

Ulrich, R., Leuthold, H., Sommer, W., 1998. Motor programming of response force and movement direction. Psychophysiology 35 (6), 721–728.

Wascher, Edmund, Arnau, Stefan, Schneider, Daniel, Hoppe, Katharina, Getzmann, Stephan, Verleger, Rolf, 2020. No effect of target probability on P3b amplitudes. Int. J. Psychophysiol. 153, 107–115. https://doi.org/10.1016/j.ijpsycho.2020.04.023.